Optical and Electrical Modeling of Three Dimensional Dye-Sensitized Solar Cells

Peijun Guo[*1], Shi Qiang Li[1], Nanjia Zhou[1], Jie Zhang[2], Robert P.H. Chang[1]
[1]Northwestern University, [2]Zhejiang University
*2220 Campus Drive, Evanston, IL, 60208, peijunguo2014@u.northwestern.edu

Abstract: Dye sensitized solar cells (DSSCs) have received tremendous attention as alternative solar energy harvesting devices due to their relatively high efficiency and cost-effectiveness. While the 10um~20um thick, sintered TiO_2 nanoparticle (NP) film attached with dye molecules achieve relatively efficient photon absorption, the photo-generated electrons have to diffuse through the thick NP film to be collected and results in high recombination losses. Three-dimensional (3D) nanostructured design could overcome the high recombination loss problem by providing shorter pathways for photo-generated electrons to reach the contact. In this work, we used COMSOL Multiphysics to simulate the optical and electrical properties of DSSCs based on both planar (2D) Indium Tin Oxide (ITO) film and periodic 3D ITO nanorod photoanodes. IV curves, quantum efficiencies, recombination profile and electron flow are calculated from the simulation. We demonstrate that the 3D nano-architecture facilitates electron transport and results in lower recombination losses and higher photocurrent.

Keywords: dye sensitized solar cells (DSSCs), optical-electrical coupled modeling, three-dimensional nanostructure, COMSOL.

1. Introduction

In the last two decades, extensive research efforts have been focused on the development of the third generation solar cells, including dye sensitized solar cells (DSSC), organic photovoltaics (OPV), quantum dot solar cells (QDSC), and etc, with the goal to achieve high efficiency with environmentally-friend materials at a much lower cost. A key challenge limiting the efficiencies of these types of solar cells, however, is short charge carrier collection distance coupled with comparatively long photon absorption length. To decouple the charge extraction and the photon absorption, nanostructures, such as nanowires, nanorods, [1] etc, have been introduced to the fabrication of 3D-architecture solar cells. The 3D nanostructures are designed to improve the charge transport of photo-generated electrons by providing them closer conducting pathways near where they are formed to the electrical contact.

The working mechanism of one of a kind 3rd generation solar cell, namely DSSC, is illustrated in Figure 1. [2] Typically, a DSSC is composed of a mesoporous TiO_2 NP film coated on transparent conducting oxide (TCO) substrate. The TiO_2 NP film is sensitized with light absorbing dye molecules, and infiltrated with a liquid electrolyte containing a redox couple, or solid-state hole transporting materials. Upon photoexcitation, electrons from the excited states of the dye molecules will be injected to the conduction band of TiO_2 NPs and further move to the front contact of the DSSC. The oxidized dye molecule is then regenerated by the redox couple, typically I/I_3^- for liquid electrolyte. The triiodide carries the holes to the Pt counter electrode and completes the circuit.

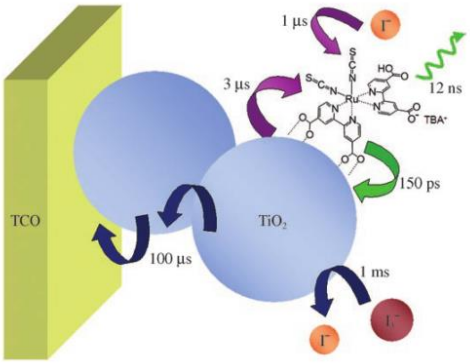

Figure 1. Kinetic processes of a typical DSSC based on TiO_2 nanoparticles attached with N719 dye molecules and iodide/triiodide redox based electrolyte. [2]

To improve the charge carrier extraction efficiency, in this work we design a periodic 3D ITO nanorod based photoanode [3] and develop a coupled optical-electrical COMSOL

Multiphysics model to simulate the physics of the DSSCs. Photoanodes made of 3D ITO nanorod architecture as well as 2D ITO film (Figure 2) are simulated and compared.

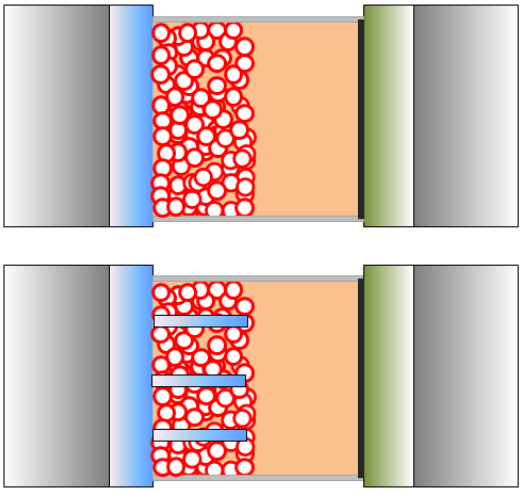

Figure 2. Illustrations of the 2D and 3D DSSC structures. (red circles: the TiO_2 NPs and the attached dye molecules on the TiO_2 surface; blue: ITO film and ITO nanorod; grey: substrate; green: fluorine doped tin oxide (FTO) film; light orange: liquid electrolyte).

2. Theory

2.1 Optical Model

The optical model is considered using the Helmholtz equation in the frequency domain with different materials represented by their refractive indexes (or, relative permittivities). Since the substrate is much thicker (about 0.5 mm) compared to the wavelength of interest, the coherence effect due to the substrate is taken into account by a generalized matrix method, [4] and is not explicitly simulated in the COMSOL model.

2.2 Electrical Model

The governing equations for the electrical modeling of DSSCs can be written as the following: [5,6]

$$\frac{\partial n_{cb}(\vec{r},t)}{\partial t} = \frac{1}{e}\frac{\partial \vec{j}(\vec{r},t)}{\partial \vec{r}} + G_e(\vec{r},t) - U_{cb}(\vec{r},t) - r_t + r_d$$

$$\frac{\partial n_t(\vec{r},t)}{\partial t} = r_t - r_d - U_t(\vec{r},t)$$

$$\vec{j}(\vec{r},t) = eD_0 \frac{\partial n_{cb}(\vec{r},t)}{\partial \vec{r}}$$

In these equations, $n_{cb}(\vec{r},t)$ is the conduction band electron density in the TiO_2 NPs, $\vec{j}(\vec{r},t)$ is the electron current flow, $G_e(\vec{r},t)$ is the generation rate of electrons by photoexcitation, $U_{cb}(\vec{r},t)$ is the recombination rate of conduction band electrons in the TiO_2 NPs, $U_t(\vec{r},t)$ is the recombination rate of trapped electron in the TiO_2 NPs, r_t is trapping rate, r_d is detrapping rate, D_0 is the conduction band electron diffusion coefficient and e is the elementary charge. Under steady state, the set of equations described above can be combined into a single diffusion equation:

$$L^2\nabla^2 n_{cb}(\vec{r}) - (n_{cb}(\vec{r}) - \bar{n}) + \tau_0 G_e(\vec{r}) = 0,$$

where $L = \sqrt{D_0\tau_0}$ is the electron diffusion length in the TiO_2 conduction band. The energy diagram and the recombination mechanisms are indicated in Figure 3. [5]

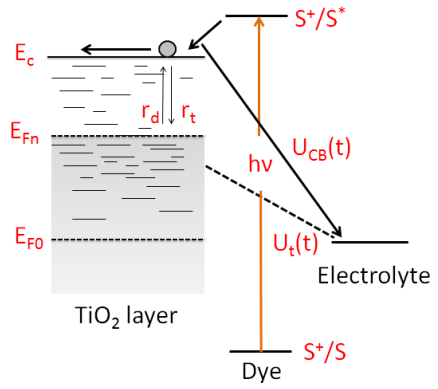

Figure 3. Energy diagram and kinetic processes of typical DSSCs.

It is assumed in the equations that the high-ionic-strength electrolyte screens the macroscopic electric field so there is no drift term for the electron flow, and the main competing process of electron transport through the TiO_2 conduction band is the interception of electrons by the I_3^- ions, with a recombination rate linear to the electron concentration in the TiO_2 conduction band. The boundary condition at the front contact (the interface between TiO_2 layer, and ITO film as well as ITO nanorod surface) is written as $n_0 = N_c \exp\left[-\left(\frac{E_c - E_{Fn}(0)}{k_B T}\right)\right]$, where n_0 is the electron concentration at the front contact, N_c is the effective density of states for electrons, E_c is the conduction band energy of the TiO_2 NPs, $E_{Fn}(0)$ is the quasi Fermi level of TiO_2 NPs at the front contact. The boundary condition at the interface between the TiO_2 layer and the electrolyte is written as $\left.\frac{dn_{cb}(\vec{r})}{dz}\right|_{z=d} = 0$, where z is the direction perpendicular to the DSC device stack. The photovoltage is represented by the equation $V = \frac{1}{e}\left(E_{Fn}(0) - E_{F0}\right)$, where E_{F0} is the Fermi level in the dark, and the photocurrent is calculated by the equation $J = \int eD_0 \frac{\partial n_{cb}(\vec{r})}{\partial \vec{r}} d\Omega$ integrated over the interface between the TiO_2 layer and the entire ITO surface (including both ITO film and ITO nanorod).

3. Use of COMSOL Multiphysics

COMSOL Multiphysics is used to build a two-step optical-electrical coupled model and the simulation flow diagram is illustrated in Figure 4. The advantage of the coupled simulation are that the 3D design of the photoanode can be straightforwardly incorporated in the model and light trapping effects can be studied as a natural extension. In addition, the unstructured grids of COMSOL enable the studying of a relatively large domain (more than 10 um^3) in visible wavelengths.

Due to the periodicity of the 3D nanostructure, the simulation domain is a unit cell containing one single nanorod. In the first step, the RF module (frequency domain) is used to model the optical response of the DSSC at each wavelength of the solar spectrum (AM 1.5), with a spectral resolution of 5 nm. The input parameters for the optical model are the geometries of the DSSC (critical parameters are the thickness of the TiO_2 layer, ITO nanorod length and spacing) and the refractive indexes of different components. The refractive indexes of the TiO_2 layer are extracted from literatures. [7] The refractive indexes of other layers, such as ITO, ZrO_2, glass, etc, are acquired from http://www.filmetrics.com/refractive-index-database. From the optical simulation result, photonic effect due to the periodic nanorod grating, maximal external quantum efficiency (EQE) and the absorption of the photo active TiO_2 layer can be studied.

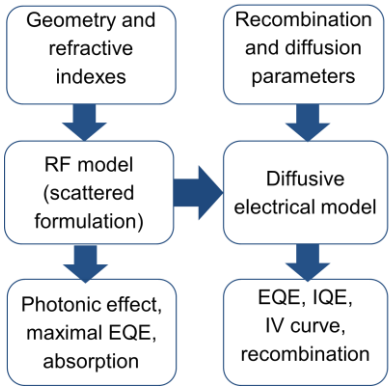

Figure 4. Two-step coupled simulation flow diagram.

A user defined port boundary condition is used to launch a plane wave with arbitrary incident angle, azimuthal angle and polarization angle. The port is defined as the following:

Ex=ux*exp(-i*(emw.k*Nkx*x+emw.k*Nky*y))

Ey=uy*exp(-i*(emw.k*Nkx*x+emw.k*Nky*y))

Ez=uz*exp(-i*(emw.k*Nkx*x+emw.k*Nky*y))

where

ux=(cos(alpha)*cos(theta)*cos(phi)-sin(alpha)*sin(phi))

uy=(cos(alpha)*cos(theta)*sin(phi)+sin(alpha)*cos(phi))

uz=-cos(alpha)*sin(theta)

Nkx=sin(theta)*cos(phi)

Nky=sin(theta)*sin(phi)

Nkz=cos(theta)

In the above equations, theta is the polar angle, phi is the azimuthal angle and alpha is the electric field polarization angle. The Floquet Boundary conditions are defined as kFx= emw.k0*Nkx in the x planes and kFy=emw.k0*Nky in the y planes. In the current work only normal incident plane wave is considered, with theta = phi = alpha = 0. The input power at each wavelength matches the AM1.5 solar spectrum. Since the periodic nanorod array can act as an optical grating, multiple reflection and transmission orders might be present at oblique incident angles. To absorb all the reflected and transmitted waves with different directions, the background field and scattered field formulation is applied. To be specific, the optical fields of the infinitely-extending multilayers are firstly calculated to provide the background fields, and the finite scattering objects in a unit cell are considered in scattered field formulation.

In the second step, the Coefficient Form PDE module (stationary) is used to model the electrical response of the DSSCs. The essential input from the optical simulation result is the generation term integrated over the solar spectrum, which is calculated from the equation $G_e(\vec{r}) = \int_{\lambda} \frac{\varepsilon(r)''|E(r)|^2 \pi}{h} d\lambda$, where λ is the wavelength of the incident light, $\varepsilon(r)''$ is the imaginary part of the permittivity of the photo active TiO2 layer, and $E(r)$ is the electric field. Other critical parameters including the diffusion length of TiO_2 conduction band electrons were extracted from literatures. [8,9]

To calculate the IV curve, a parametric sweep of $E_{Fn}(0)$, the quasi Fermi level of TiO_2 NPs at the front contact, is performed. The photovoltage and the photocurrent are then calculated as described in section 2. To obtain the EQE and IQE curve, the generation rate of electrons is calculated at each wavelength with subsequent photocurrent calculations at short circuit conditions. The EQE is computed through dividing the number of generated electrons by the number of photons of the monochromatic light, and the IQE is computed by dividing the number of extracted electrons by the number of photons absorbed by the TiO_2 layer.

4. Simulation Result

Figure 5 shows the IV curves of DSSCs made of 2D and 3D ITO photoanodes. It is observed that 3D nanostructure gives a photocurrent enhancement of about 20%. Figure 6 shows the EQE and IQE curves of the same. It can be seen that the 3D nanostructured photoanodes provide better photon-to-electron conversion efficiency especially at long wavelengths. This is due to a weak absorption coefficient of the dye molecule at these long wavelengths. The photo-generated electrons have a larger distribution at the TiO_2 layer far from the front contact, and as a result the 3D nanostructures could make improvements by providing shorter pathways for these electrons.

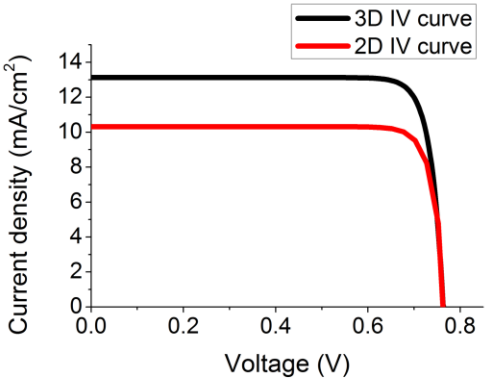

Figure 5. I-V curves of 2D and 3D DSSCs.

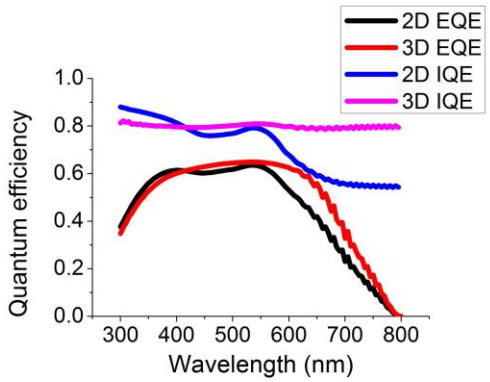

Figure 6. EQE and IQE curves of 2D and 3D DSSCs.

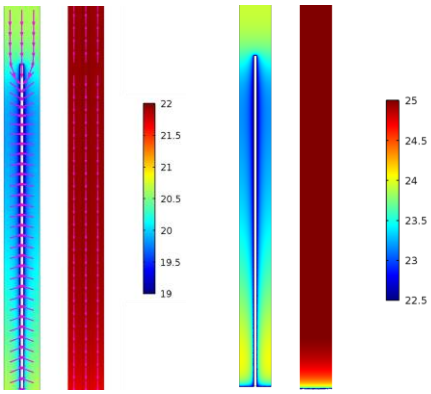

Figure 7. Left two: electron concentration on $\log_{10}$ scale ($1/m^3$) and electron flow at short circuit condition; Right two: recombination profile on $\log_{10}$ scale ($1/m^3/s$) at short circuit condition. The ITO nanorod is shown as the white vertical rod inside the simulation domain. In each set of the figures the 3D result is firstly showed followed by the 2D counterpart.

Figure 7 shows the electron concentration, as well as the recombination of the electrons at the center cross section of a unit cell of the device simulated. The electron flow is calculated as the gradient of the electron concentration in the TiO_2 conduction band. It is clear that the electrons flow horizontally to the nearby ITO nanorod surface in 3D case, instead of flow vertically to the front contact in the case of using 2D ITO film photoanode. This results in a much lower conduction band electron concentration (shown in the left of Figure 7) as well as a much lower recombination rate (shown in the right of Figure 7).

4. Conclusions

We have used a two-step optical–electrical coupled COMSOL Multiphysics model to simulate the performances of DSSCs based on both 2D and 3D ITO photoanodes. Useful information such as IV curve, EQE, IQE, electron flow and recombination profile have been extracted. It is demonstrated that the advantage of the 3D electrode design comparing to its 2D counterpart is lower recombination losses due to a shorter charge carrier transport length to the electrical contact. As a result, a higher short circuit current is obtained, together with higher energy conversion efficiency.

A systematic variation of the device geometries, such as the TiO_2 layer thickness, nanorod length, nanorod spacing is being studied with the goal of achieving optimized efficiency. Experiments of the same are currently underway and initial results compare well qualitatively with the simulation results. In addition, this model is now being expanded to include both diffusion and drift currents which will enable the simulation of all solid state DSSC, [10] and potentially organic solar cells with complex nanoscale morphologies. [11]

5. References

1. Shi Qiang Li, Peijun Guo, Lingxiao Zhang, Wei Zhou, Teri W. Odom, Tamar Seideman, John B. Ketterson and Robert P.H. Chang, Infrared Plasmonics with Indium-Tin-Oxide Nanorod Arrays, *ACS Nano*, **5**, 9161-9170 (2011)
2. Alex Martinson, Thomas Hamann, Michael Pellin, Joseph Hupp, New Architectures for Dye-Sensitized Solar Cells, *Chemistry*, **14**, 4458-4467 (2008)
3. Byunghong Lee*, Peijun Guo*, Shi Qiang Li, D, Bruce Buchholz, R. P. H. Chang, 3D indium-tin-oxide nanorod array for charge collection in dye sensitized solar cells, *submitted* (* equal contribution)
4. E. Centurioni, Generalized Matrix Method for Calculation of Internal Light Energy Flux in Mixed Coherent and Incoherent Multilayers, *Applied Optics*, **44**, 7532-7539 (2005)
5. L. M. Peter, Characterization and Modeling of Dye-Sensitized Solar Cells, *The Journal of Physical Chemistry C*, **111**, 6601-6612 (2007)

6. Sophie Wenger, Matthias Schmid, Guido Rothenberger, Adrian Gentsch, Michael Gratzel and Jurgen O. Schumacher, Coupled Optical and Electronic Modeling of Dye-Sensitized Solar Cells for Steady-State Parameter Extraction, *The Journal of Physical Chemistry C*, **115**, 10218-10229 (2011)
7. Guido Rothenberger, Pascal Comte and Michael Gratzel, A Contribution to the Optical Design of Dye-Sensitized Nanocrystalline Solar Cells, *Solar Energy Materials & Solar Cells*, **58**, 321-336 (1999)
8. Piers R. F. Barnes, Assaf Y. Anderson, Sara E. Koops, James R. Durrant and Brian C. O'Regan, Electron Injection Efficiency and Diffusion Lengths in Dye-Sensitized Solar Cells Derived from Incident Photon Conversion Efficiency Measurements, *The Journal of Physical Chemistry C*, **113**, 1126-1136 (2009)
9. Byunghong Lee, Dae-Kue Hwang, Peijun Guo, Shu-Te Ho, D. B. Buchholtz, Chiu-Yen Wang and Robert P.H. Chang, Materials, Interfaces, and Photon Confinement in Dye-Sensitized Solar Cells, *The Journal of Physical Chemistry B*, **114**, 14582-14591 (2010)
10. Byunghong Lee, D. B. Buchholz, Peijun Guo, Dae-Kue Hwang and Robert P.H. Chang, Optimizing the Performance of a Plastic Dye-Sensitized Solar Cell, *The Journal of Physical Chemistry C*, **115**, 9787-9796 (2011)
11. Nanjia Zhou, Hui Lin, Sylvia J. Lou, Xinge Yu, Peijun Guo, Eric F. Manley, Stephen Loser, Patrick Hartnett, Hui Huang, Michael R. Wasielewski, Lin X. Chen, Robert P.H. Chang, Antonio Facchetti and Tobin J. Marks, Morphology-Performance Relationships in High-Efficiency All-Polymer Solar Cells, *Advanced Energy Materials*, Early View, (2013)

6. Acknowledgements

We would like to thank Dr. Pierfrancesco Zilio and Dr. Lynn An for numerous discussions on the optical modeling using COMSOL, and Dr. Alex Martinson for insightful discussions on the electrical modeling of the DSSCs.

7. Appendix

Table 1: Parameters used in the calculations

Electron diffusion length in TiO_2 conduction band	10 microns
ITO film thickness	200 nm
ITO nanorod length	13 um
ITO nanorod side length	100 nm
ITO nanorod periodic spacing	1.2 um
TiO_2 film thickness	15 um